A FTIR and 2D-IR Spectroscopic Study on the Microdynamics Phase Separation Mechanism of the Poly(*N*-isopropylacrylamide) Aqueous Solution

Bingjie Sun,[†] Yinan Lin,[†] Peiyi Wu,*[,†] and Heinz W. Siesler[‡]

The Key Laboratory of Molecular Engineering of Polymers (Ministry of Education) and Department of Macromolecular Science and Advanced Materials Laboratory, Fudan University, Shanghai 200433, PR China, and Department of Physical Chemistry, University of Duisburg-Essen, D 45117 Essen, Germany

Received September 13, 2007; Revised Manuscript Received December 11, 2007

ABSTRACT: The thermal behavior of PNIPAM in its concentrated D_2O solution (20 wt %) was studied by FTIR and 2D-IR correlation spectroscopy. The spectral data of the C−H groups and the Amide I region provide details about the changes of the hydrophobic and hydrophilic parts in the polymer respectively during a heating−cooling cycle. The reversal of peak positions of the C−H bands upon cooling indicates the reversibility of temperature-induced dehydration of the hydrophobic groups. The change in hydrogen bonding of C═O···D−N constructed between dehydrated C═O and N−D groups, as derived from the Amide I region, does not revert precisely in the cooling process due to the newly formed hydrogen bonds in the collapsed state, and a hysteresis phenomenon is observed. In our concentrated solution (20 wt %), the strength of those intra- and interchain hydrogen bonds even prevent the polymers from dissociating completely below the LCST during the cooling process. The microdynamics phase separation mechanism was obtained by application of the 2D-IR analysis to the spectral data. When the temperature rises, the two-step dehydration of the CH_3 groups occurs first, then the main-chain diffusion and aggregation takes place, and finally the hydrogen bond transition occurs. The dynamic sequence in the cooling process is also described.

Introduction

Poly(*N*-isopropylacrylamide) (PNIPAM), is a polymer sensitive to different environmental variations such as temperature,[1−14] and it is especially popular in the application of drug release,[15] peptides separation,[16] and surface modification.[17]

It is generally believed that two species of water exist within the PNIPAM polymer when it is dissolved in an aqueous solvent, that is the free and bound water.[18,19] The presence of the bound water can be also divided into two species, one is related to form the hydrogen bonds with some C═O or NH groups;[20,21] the other is related to interact with the hydrophobic groups like the methyl groups or the main-chain hydrocarbons.[21−26] This kind of hydration interaction has the same range as, but is about an order of magnitude stronger than, the van der Waals-dispersion force,[23] and it is considered to be a complex result of the tendency of hydrophobic molecules to minimize the interface with water molecules and the corresponding entropy change of water around the hydrophobic groups.[22,23] Saito et al.[24,25] introduced the concept of "water cage" around the isopropyl group on the side chains of PNIPAM, and Cho et al.[26] drew the configuration of such "water cage", making the interaction between the hydrophobic groups and the water molecules much clearer. PNIPAM undergoes reversible coil-to-globule transition, after which the chains collapse and aggregate into bigger globules,[20] in water above its lower critical solution temperature (LCST ∼ 32 °C).[20,21] The dehydration of the hydrophobic groups together with the changes of hydrogen bonds containing the hydrophilic groups induces the coil-to-globule transition of the polymer.

A great deal of research[12−14,20,21,27−30] has been done to investigate the temperature dependence behavior of PNIPAM, and many techniques such as light scattering,[20] DSC,[5] calorimetry,[31,32] fluorescence,[33,34] turbidimetry,[35] nuclear magnetic resonance,[36] and Raman spectroscopy[37] were used. Among them IR spectroscopy is an effective method used to investigate the changes in conformation, interaction, and microenvironment of the individual chemical groups in the PNIPAM phase transition.[21,28,38,39] Ozaki et al.[38,39] discovered changes in the amide bands during heating, and pointed out that the hydration of the amide groups and the changes of the C═O···H−N hydrogen bonds may cause the spectral variations. Meada et al.[21,28] observed that most of the carbonyl groups form hydrogen bonds with water molecules in the coiled state, but 13% of the C═O groups would be bound to the N−H groups in the globular state. They have also found that due to the dehydration of the isopropyl side chain and the main chain of PNIPAM, the C−H stretching IR bands shift to lower wavenumbers during the heating process. Chi Wu et al.[20] used LLS and IR spectroscopy to investigate the heating-and-cooling cycle of dilute aqueous PNIPAM solutions, showing that, in addition to a hysteresis due to the hydrogen bonds between different overlapped segments in the collapsed state, the formation and rupture of the C═O···D−N was reversible in the coil-to-globule-to-coil transition process.

Generalized two-dimensional (2D) correlation spectroscopy, a technique originally proposed by Noda[40−42] in 1993, enables the investigation of the spectral intensity fluctuation under a disturbing variable which can be temperature,[43,44] time,[45,46] pH,[47] or concentration[48] etc. The specific event sequence of the system in the perturbing process can thus be understood. 2D spectra can capture subtle information which is not obvious in 1D spectra due to spreading the peaks over the second dimension thereby improving the spectral resolution.

* Corresponding author: E-mail: Peiyiwu@fudan.edu.cn.
[†] The Key Laboratory of Molecular Engineering of Polymers (Ministry of Education) and Department of Macromolecular Science and Advanced Materials Laboratory, Fudan University.
[‡] Department of Physical Chemistry, University of Duisburg-Essen.

10.1021/ma702062h CCC: $40.75
Published on Web 01/23/2008

Despite the widespread application of FTIR spectroscopy for research on the PNIPAM LCST behavior, the precise quantitative analysis of the changes in the C−H spectral region is still lacking, and the studies of the amide I region were focused on the heating process only, additionally, the accurate conclusion about the thermal induced phase separation microdynamics mechanism of PNIPAM still remains a blank. In the present study, the peak positions of the hydrophobic groups on the PNIPAM chains are analyzed quantitatively for the first time, and 2D-IR correlation spectroscopy serves as a new and useful technique when studying the temperature-dependent microdynamics mechanism of PNIPAM in the heating-and-cooling cycle.

Experimental Section

Sample Preparation. *N*-Isopropylacylamide (NIPAM) monomers were purchased from Tokyo Kasei Kogyo Co. (Tokyo, Japan). Poly-NIPAM was synthesized by free-radical polymerization in *tert*-amyl alcohol as solvent. The reaction was initiated by azobis (isobutyronitrile) (AIBN) and carried out at 70 °C for 12 h under a nitrogen atmosphere. The precooled reaction solution was dropped slowly into a large volume of pure diethyl ether. The precipitate was then dried under vacuum to constant weight. The synthetic polymer has a melting point of 220 °C as determined by differential scanning calorimetry (DSC). The molecular weight of PNIPAM, $M_w = 5220$, and polydispersity index, $M_w/M_n = 1.18$, were measured by a Voyager DE-STR matrix-assisted laser desorption/ionization time-of-flight (MALDI−TOF MS) mass spectrometer equipped with a 337 nm nitrogen laser. The instrument was calibrated with Angiotensin and Insulin and operated in the reflector mode. Samples were prepared by mixing the solution of PNIPAM (8μL, 10 mg/mL in THF), the matrix (8μL, 10 mg/mL in DHB/THF), and $NaBF_4/CH_3OH$ (Ionization agent, 2μL). According to the molecular weight, it seems that PNIPAM polymerized by this method is an oligomer.

PNIPAM was dissolved in heavy water (Cambridge Isotope Laboratories, Inc., D-99.9%) with a concentration of 20.0 wt % and the solution was kept for 1 week before experiments in order to ensure the complete deuteration of all the NH protons.

Fourier Transform Infrared Spectroscopy. The FTIR spectra were recorded with a 4 cm^{-1} spectral resolution on a Nicolet Nexus 470 spectrometer equipped with a DTGS detector by signal-averaging 64 scans. Two pieces of microscope CaF_2 windows, which have no absorption bands in the MIR region were used to prepare a transmission cell. Variable-temperature spectra were collected between 28 and 40 °C with an increment of 1 °C (accuracy: 0.1 °C). Manual method was used to change the temperature, each temperature point was maintained for 30 min to collect the IR spectrum, and then the temperature was increased or decreased for 1 °C manually. The baseline correct processing was performed by the software of OMNIC 6.1.

Two-Dimensional Correlation Analysis. Spectra recorded at an interval of 1 °C were selected in certain wavenumber ranges and the generalized 2D correlation analysis was applied by the 2D Shige software composed by Shigeaki Morita (Kwansei-Gakuin University, Japan). The 2D correlation spectrum is shown in the center of the map, while the averaged 1D reference spectrum is at the side and the top. In the 2D correlation maps, the red-colored regions are defined as the positive correlation intensities, whereas the blue-colored ones are regarded as the negative correlation intensities.

Results and Discussion

D_2O, rather than H_2O, was used here as the solvent to eliminate the overlap of the δ(OH) band of water at about 1640 cm^{-1} with the ν(C═O) band of PNIPAM. Many researchers[2−4,49−53] have reported the isotope effect between PNIPAM aqueous solution and deuterated PNIPAM aqueous solution, the results

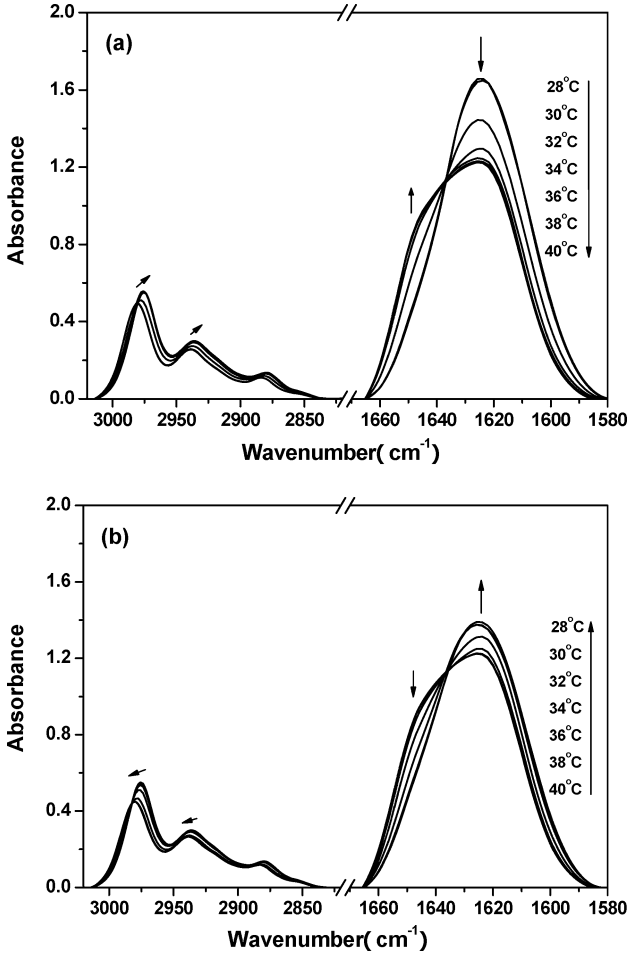

Figure 1. FTIR spectra of PNIPAM 20 wt % D_2O solution as a function of temperature: during heating (a) and cooling (b). The temperature was varied between 28 and 40 °C with an interval of 2 °C.

of those studies showing the influence on the thermal behavior. (i) The LCST of PNIPAM in D_2O is about 0.7 °C higher than in H_2O.[2] (ii) The magnitudes of the hysteresis of the transition temperatures (the difference between the transition temperatures in the heating process and the cooling process) are not affected or are only weakly affected by isotopic substitutions.[2] We have also worked on the PNIPAM 20 wt % H_2O solution before, the dehydration course of the CH groups and the heating-and-cooling process are almost of the same condition with the PNIPAM 20 wt % D_2O solution, however the overlap of the band of water and PNIPAM enhanced the difficulties and blocked the FTIR research; besides, the LCST was a little different between the two kinds of PNIPAM solutions according to the DSC results (32.1 °C in PNIPAM 20% D_2O solution and 31.3 °C in PNIPAM 20% H_2O solution).

Figure 1a shows the temperature dependence of the absorption bands of the C−H and C═O groups of PNIPAM in 20 wt % D_2O solution (28−40 °C cycle). For clarity, not all the spectra are shown in Figure 1a. The absorption bands centered at about 2981, 2938, 1649, and 1624 cm^{-1} can be attributed to the vibration of $\nu_{as}(CH_3)$ of the side chains of PNIPAM,[21,54] $\nu_{as}(CH_2)$ of the main chains,[21,54] Amide I (C═O hydrogen bonded with N−D),[20,21,28] and Amide I (C═O hydrogen bonded with D−O−D),[20,21,28] respectively. In accordance with the equation −NH(of PNIPAM) + $D_2O \rightleftharpoons$ −ND + HDO, however, there may be some other species in the solution after deuterium substitution of PNIPAM with heavy water, like HDO, and the reverse chemical exchange could happen between −ND and H (of HDO) as well, therefore the deuterium substitution for

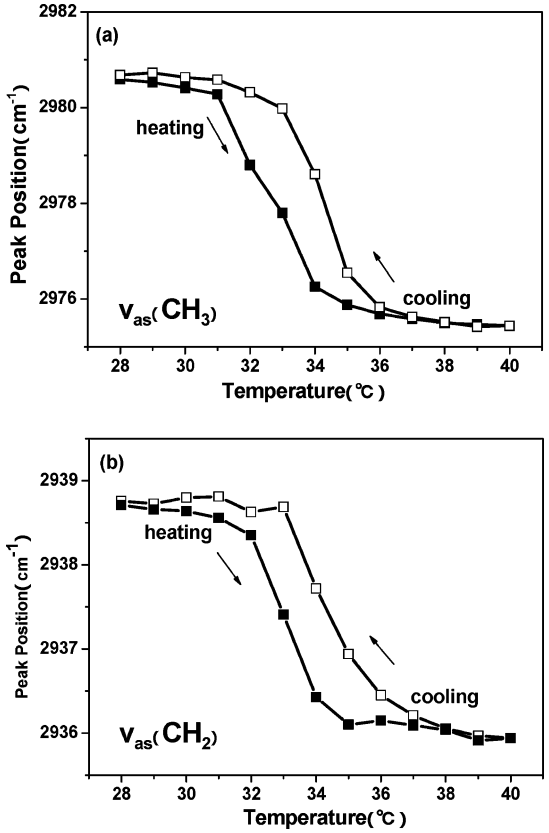

Figure 2. Peak position of $v_{as}(CH_3)$ (a) and $v_{as}(CH_2)$ (b) in the FTIR spectra of PNIPAM 20 wt % D_2O solution as a function of temperature. The temperature of the heating−cooling cycle was varied between 28 and 40 °C with an interval of 1 °C. Filled symbols show the heating process, and open symbols show the cooling process.

PNIPAM in D_2O solution cannot be complete. Moreover, the H atom (in −NH or HDO) and the D atom (in HDO) may also form hydrogen bonds with the carbonyl groups, which would greatly increase the complication of the research. After calculation, nevertheless, the ratio of the number of H (in −NH of PNIPAM) to the number of D_2O (in PNIPAM 20 wt %(weight percent) D_2O solution) is 1:20. This reveals that there are far more D_2O than H (in −NH of PNIPAM) in our research system, thus the deuterium substitution equation mentioned above would mainly happen toward the right direction, and the limited number of HDO can be nearly neglected.

The main spectral changes during the heating process in Figure 1a can be summarized as follows: (1) The bands of $v_{as}(CH_3)$ and $v_{as}(CH_2)$ shift to lower wavenumbers. (2) The intensity of the band at 1624 cm^{-1} remains constant at room temperature, but above LCST, it decreases while the intensity of the 1649 cm^{-1} band increases. As the bands of 1624 and 1649 cm^{-1} are assigned to the hydrogen bonds of C═O···D−O−D and C═O···N−D,[20,21,28] respectively, this evidence confirms that when PNIPAM chains go through the coil-to-globule transition, their C═O groups dehydrate and new hydrogen bonds (C═O hydrogen bonded with N−D) form.

In Figure 1b, when the temperature drops, there's a blue shift concerning the bands of $v_{as}(CH_3)$ and $v_{as}(CH_2)$ together with an intensity decrease at about 1649 cm^{-1} and an intensity increase at 1624 cm^{-1}, which is opposite to the changes upon heating.

In Figure 2, the band shifts of $v_{as}(CH_3)$ and $v_{as}(CH_2)$ have been monitored during the temperature cycle. At the beginning of heating, both peaks shift only slightly to lower wavenumbers, while this red shift significantly increases above the LCST. In the cooling process, the starting point of the blue shift is located at 40 °C, around the LCST these peaks shift largely and finally both peaks could return to their original high wavenumbers. It is well-known that the peak shifts during heating reveal the dehydration of the CH_3 and CH_2 groups, and the shifts during cooling manifest the hydration effect between the C−H groups and the D_2O molecules in solution.[55] Furthermore, in the heating−cooling cycle, the transition temperature of the CH_3 groups on the PNIPAM side chains can be observed slightly lower (at about 32 °C) than that of the CH_2 group on the main chains (at 33 °C), which suggests that the CH_3 group changes prior to the CH_2 group. This observation indicates that the side chains are more sensitive to the temperature than the main chains, and it is consistent with the conclusion we have gained in the analysis of PNIPAM film before.[54]

As pointed out before, the use of D_2O as solvent is beneficial for the study of the Amide I area, and the limited incomplete deuteration effect can be neglected. The two species of the carbonyl hydrogen bonds can then be easily analyzed by means of curve fitting. Below the LCST, the Amide I band only consists of a single Gaussian component centered at about 1624 cm^{-1} assigned to the hydrogen bond formed by C═O···D−O−D.[20,21,28] While the other component, centered at about 1649 cm^{-1} and attributed to the C═O···D−N hydrogen bond,[20,21,28] appears above the LCST. Presuming a 1:1 conversion of the carbonyls,[21] when the peak area of one component is plotted as a function of the other component, the slope of the fitted line, 0.91, yields the ratio of the molar absorptivity of C═O··D−N relative to that of C═O···D−O−D (Figure 3a). Figure 3b shows the temperature dependence of the molar fraction f(C═O···D−N) in the temperature cycle, in which f(C═O···D−N) is defined as A1649/[A1649 + A1625*(ϵ1649/ϵ1625)].

According to Figure 3b, during heating, the value of f(C═O···D−N) remains zero until the temperature reaches the LCST of PNIPAM aqueous solution. This plateau corroborates that the hydrogen bonding of C═O···D−N only forms above 32 °C, because PNIPAM chains do not start to dehydrate, aggregate and collapse below its LCST. The C═O and N−D groups without hydration interact with each other and form new entropically preferred[20] C═O···D−N hydrogen bonds. In addition, it can be observed that only 34.7% of the C═O groups form hydrogen bonds with the N−D groups after phase separation, while the remaining 65.3% sustain their hydrogen-bond relationship with water, which clarifies that only a small fraction of the C═O···D−O−D hydrogen bonds are destroyed during the coil-to-globule transition, and there's still a lot of water retained in the concentrated phase of the separated system. In Figure 3b, a apparent hysteresis is noticed. When the temperature drops, the value of f(C═O···D−N) decreases, but it is always larger than the value during the heating process. It is widely known that the hysteresis is due to the formation of the hydrogen bonds between different overlapped chains in the collapsed state, and such hydrogen bonds cannot be easily removed in the cooling process.[20] However, different from the dilute solutions, in this case, the value of f(C═O···D−N) does not turn back to zero even when the temperature is far below the LCST. The concentration of the deuterated aqueous PNIPAM solution, 20 wt %, may provide an explanation for this result: the much more entangled chains and the much stronger C═O··D−N hydrogen-bond interactions than those in the dilute solution prevent the system from reversing to its original state.

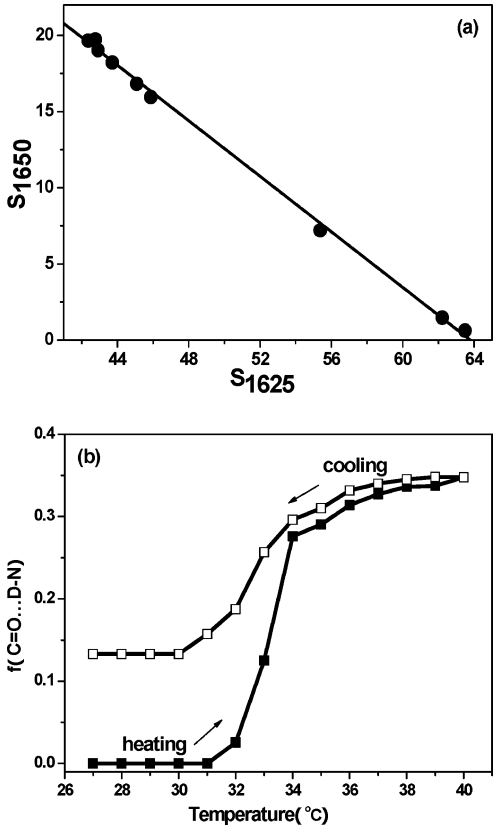

Figure 3. (a) Relative areas of 1650 cm^{-1} of the C═O···D−N hydrogen bonding in PNIPAM 20 wt % D_2O solution at different temperatures (from 32 to 40 °C) are plotted against the areas of the 1625 cm^{-1} component (C═O···D−O−D hydrogen bonding). The slope of the fitting line yields the ratio of the molar absorption coefficient (ϵ1650/ϵ1625) as 0.91. (b) Temperature dependence of the molar fractions f(C═O···D−N) of the PNIPAM 20 wt % D_2O solution in the heating−cooling cycle (between 28 and 40 °C with an interval of 1 °C). Filled symbols show the heating process, and open symbols show the cooling process.

Two-Dimensional Correlation Analysis of the Heating Process

The red-colored and blue-colored areas in the 2D-IR correlation contour maps represent positive and negative cross-peaks respectively throughout this paper. The 2D-IR correlation spectra are characterized by two independent wavenumber axes (ν_1, ν_2) and a correlation intensity axis. Two types of spectra, 2D synchronous and asynchronous spectrum are obtained in general. The correlation intensity in the 2D synchronous and asynchronous maps reflects the relative degree of in-phase or out-of phase response, respectively.

The 2D synchronous spectra are symmetric with respect to the diagonal line in the correlation map. Some peaks appearing along the diagonal are called the autopeaks, and the symbols of them are always positive, as autopeaks represent the degree of autocorrelation of perturbation-induced molecular vibrations. Where the autopeak appears, the peak at this wavenumber would change greatly under environmental perturbation. Off-diagonal peaks, named cross-peaks ($\Phi(\nu_1, \nu_2)$), may be positive or negative, which represent the simultaneous or coincidental changes of spectra intensity variations measured at ν_1 and ν_2. Positive cross-peaks (the symbol of $\Phi(\nu_1, \nu_2)$ is positive) demonstrates the intensity variations of the two peaks at ν_1 and ν_2 are taking place in the same direction (both increase or both decrease) under the environmental perturbation; while the negative cross-peaks (the symbol of $\Phi(\nu_1, \nu_2)$ is negative) help to infer that the intensities of the two peaks at ν_1 and ν_2 change in opposite directions (one increases, while the other one decreases) under perturbation.

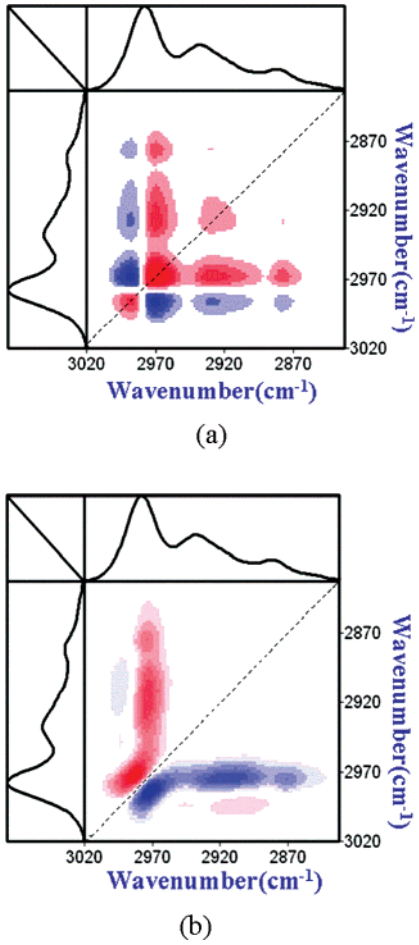

Figure 4. Synchronous (a) and asynchronous (b) maps of the PNIPAM 20 wt % D_2O solution in the region 3020−2830 cm^{-1} representing the heating process.

The 2D asynchronous spectra are asymmetric with respect to the diagonal line in the correlation map. Unlike synchronous spectra, only off-diagonal cross-peaks would appear in asynchronous spectra, and these cross-peaks can also be either positive or negative. The intensity of the asynchronous spectrum ($\Psi(\nu_1, \nu_2)$) represents sequential or successive changes of spectral intensities observed at ν_1 and ν_2. With the cross-peaks both in synchronous and asynchronous maps, we can get the specific order of the spectral intensity changes taking place while the sample is subjected to an environmental perturbation. According to Noda's rule,[40−42] when $\Phi(\nu_1, \nu_2) > 0$, if $\Psi(\nu_1, \nu_2)$ is positive (red-colored area), band ν_1 will vary prior to band ν_2; if $\Psi(\nu_1, \nu_2)$ is negative (blue-colored area), band ν_1 will vary after ν_2. However, this rule is reversed when $\Phi(\nu_1, \nu_2) < 0$. Be brief, if the symbols of the cross-peak in the synchronous and asynchronous maps are the same (both positive or both negative), band ν_1 will vary prior to band ν_2; While if the symbols of the cross-peak are different in the synchronous and asynchronous spectra (one positive, and the other one is negative), band ν_1 will vary after ν_2 under the environmental perturbation.

A. The C—H Region. The synchronous and asynchronous maps for the heating process of the PNIPAM 20 wt % D_2O solution in the 3020−2830 cm^{-1} region are shown in Figure 4. In the synchronous map (Figure 4a), two strong autopeaks develop at 2970 and 2927 cm^{-1}, which point out the prominent changes of these two peaks with temperature elevation. The

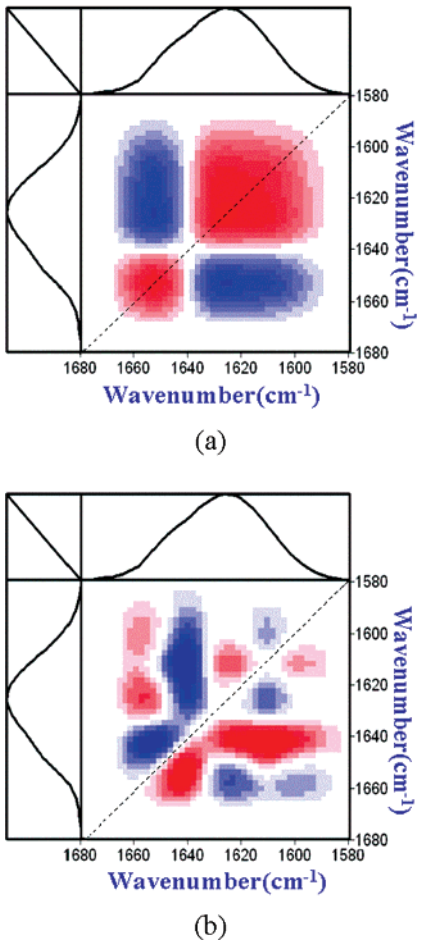

Figure 5. Synchronous (a) and asynchronous (b) maps of the PNIPAM 20 wt % D_2O solution in the region 1680−1580 cm^{-1} during the heating process.

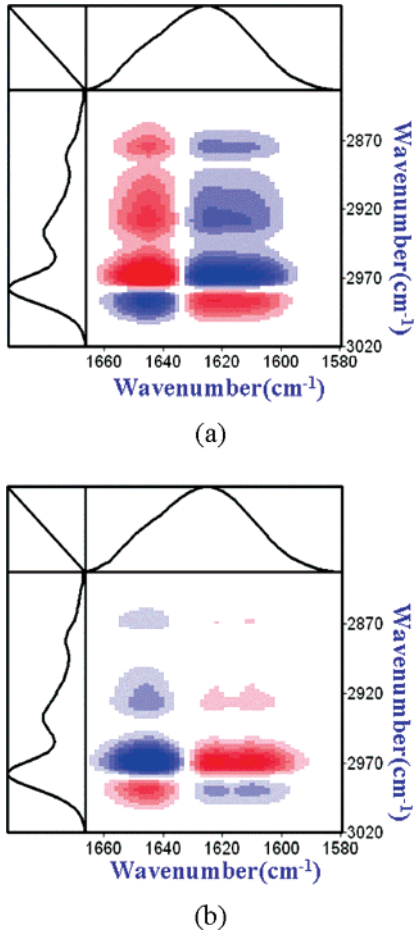

Figure 6. Synchronous (a) and asynchronous (b) maps of the PNIPAM 20 wt % D_2O solution in the regions 1670−1580 and 3020−2830 cm^{-1} during the heating process.

positive cross-peak at (2970, 2927) cm^{-1} points that the heating-induced intensity variations of the above two peaks 2970 and 2927 cm^{-1} are taking place in the same direction.

The asynchronous 2D-IR correlation spectrum, shown in Figure 4b, is asymmetric with respect to the diagonal line. The positive cross-peak at (2970, 2927) cm^{-1} implies that out-of-phase spectral changes occur at the two wavenumbers.[40] As explained by the rule put forward by Noda,[40−42] the symbols of the cross-peak at (2970, 2927) cm^{-1} are both positive in the synchronous and asynchronous maps, infers that when heated, the intensity of the 2970 cm^{-1} band varies prior to that of the 2927 cm^{-1} band. Another positive cross-peak centered at (2981, 2970) cm^{-1} could also be identified in Figure 4b, and the symbol at that center point is judged to be positive through the slice spectrum of the synchronous map. This proves that the peak at 2981 cm^{-1} changes before the one at about 2970 cm^{-1}. In total, the cross-peaks at (2970, 2927) and (2981, 2970) cm^{-1} in the 2D maps finally help to conclude the changing sequence of the three bands observed in the spectra as 2981 > 2970 > 2927 cm^{-1}. (The symbol ">" means change prior to)

In the 1D-IR spectra, the peak of $\upsilon_{as}(CH_3)$ lies at about 2981 cm^{-1} at room temperature and performs red-shift upon heating. As mentioned above, these hydrophobic side-chain groups reflect the hydration effect in solution, and the more the water molecules surrounds the polymer, the higher the wavenumber of the CH stretching vibration is.[55] It is widely known that the bands of the CH groups will perform red shifts during heating, which reveals the dehydration of the CH_3 and CH_2 groups;[21] while in the cooling process, the blue shifts of the peaks manifest the hydration effect between the C−H groups and the D_2O molecules in solution. Additionally, in Figure 1a, the apparent peak position of the CH_3 group is shifting without intensity changes (after baseline correction) as the temperature rises, thus we can mainly conclude that the peak shift is only caused by the change of the species of the hydrated methyl groups, and further ascribe the peak at 2981 cm^{-1} to the vibration of the CH_3 groups interacting with a greater number of D_2O molecules; and the peak at 2970 cm^{-1} to the vibration of less hydrated CH_3 groups.

Moreover, the shape of the cross-peak at (2981, 2970) cm^{-1} is different from the butterfly pattern only caused by the peak shift effect proposed by Noda and Ozaki.[56] Hence, the two peaks at 2981 and 2970 cm^{-1} can be again attributed to the vibration of the CH_3 groups interacting with more or less numbers of D_2O molecules, respectively. With the peaks located at 2981 and 2970 cm^{-1}, 2D-IR spectroscopy, therefore, testifies the two-step dehydration of the side-chain CH_3 groups in the temperature-elevation process. According to the sequence gained in the 2D-IR maps: 2981 > 2970 cm^{-1}, the changes of the hydration effects of the CH_3 groups can be clearly observed, which will change with two dehydration steps during heating: the CH_3 groups hydrated with more water molecules (2981 cm^{-1}) will first change to the less hydrated CH_3 groups (2970 cm^{-1}) with the first step dehydration process, then this less hydrated CH_3 groups (2970 cm^{-1}) will further dehydrated with a second step (the band of the vibration of methyl groups without hydration interaction with water exists at 2968 cm^{-1}).[54]

Scheme 1. Dynamics of the Functional Groups in PNIPAM 20 wt % D_2O Solution during Temperature Increase[a]

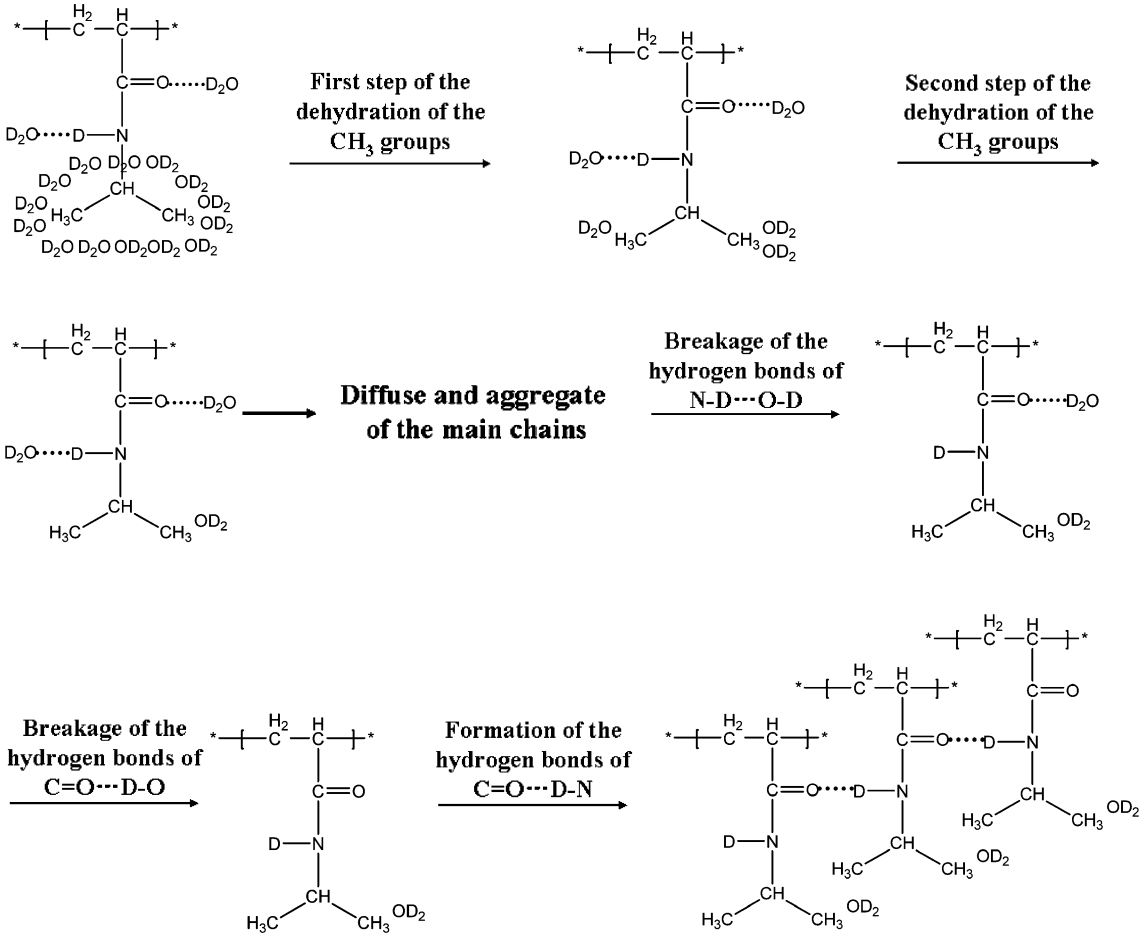

[a] The number of the water molecules that surround the methyl groups and form the "water cage" is not exact; it is only an approximate figure to show the two-step dehydration process of the CH_3 groups.

On the other hand, the changes regarding the $\upsilon_{as}(CH_2)$ peak of the stretching vibration of the CH_2 group in the main chains may reflect the movements (diffusion and aggregation in the heating process) of the main chains. Furthermore, the event sequence 2981 > 2970 > 2927 cm^{-1} supports that for the PNIPAM C−H groups during heating, the two-step side-chain dehydration first emerges and then the main-chain aggregation follows. This conclusion is consistent with the one gained by 1D-IR and the inference in the study of PNIPAM film.[54]

B. The Amide I Region. The synchronous 2D-IR spectrum (Figure 5a) in the 1680−1580 cm^{-1} range is dominated by two strong autopeaks at 1649 and 1624 cm^{-1} and a negative cross-peak at (1649, 1624) cm^{-1}. The above two autopeaks are attributed to the vibrations of the C═O···D−N and C═O···D−O−D hydrogen bonds, respectively.[20,21,28] As it is negative in the synchronous map, the cross-peak of (1649, 1624) cm^{-1} helps to infer that the two species of carbonyl hydrogen bonds transform in opposite directions (one increases, while the other one decreases) during heating. Furthermore, with the positive cross-peak at (1649, 1624) cm^{-1} in the asynchronous map of Figure 5b, Noda's rule[40−42] can help to conclude that the peak of 1624 cm^{-1} alters before that of 1649 cm^{-1} when temperature rises, which means that the change of the C═O···D−O−D is prior to the C═O···D−N hydrogen bonding. The carbonyl will first run out of the hydrogen bonds of C═O···D−O−D and then will further form the new C═O···D−N hydrogen bonding with D−N group. There are also several minor cross-peaks in the asynchronous map, probably are due to the hydrogen bonds between the limited HDO or incompletely deuterated −NH (of PNIPAM) and carbonyl groups, however assignments of these bands were less definite, and these tiny cross-peaks do not influence the main peaks investigated by us.

C. Amide I Region vs the C—H Region. This part of the analysis which correlates the 1670−1580 cm^{-1} region with the 3020−2830 cm^{-1} region (in Figure 6) provides a macroscopic view of the whole phase separation process of PNIPAM. The cross-peak at (1624, 2929) cm^{-1} can be observed in both 2D maps, the symbol of this peak is negative in the synchronous and positive in the asynchronous maps, thus we can infer the change order of 2929 > 1624 cm^{-1} in heating. The sequence gained above in the 2D analysis of the CH region and the amide I is 2981 > 2970 > 2929 cm^{-1} and 1624 > 1649 cm^{-1}, respectively. Therefore, with the order we get in this part C: 2929 > 1624 cm^{-1}, the transition sequence of all the peaks can be linked as 2981 > 2970 > 2929 > 1624 > 1649 cm^{-1}. Other cross-peaks in Figure 6 also validate this whole order of the changes of peaks. Nevertheless, more considerations are still needed to include the information about the N−D groups into the above sequence. From the perspective of using the spectra density method[57] (where the spectral density is obtained from the Fourier transform of the translational velocity autocorrelation function, and it can help to obtain the information about the local motion of water molecules in the solution), both, the formation and destruction of the hydrogen bonds between N−H and water take place on a very short time scale, faster than the C═O···H−O−H hydrogen bonds.[57] Otherwise, as detailed in the explanation of Figure 2 and 3, the hydrophobic groups dehydrate almost as soon as the temperature elevates. The

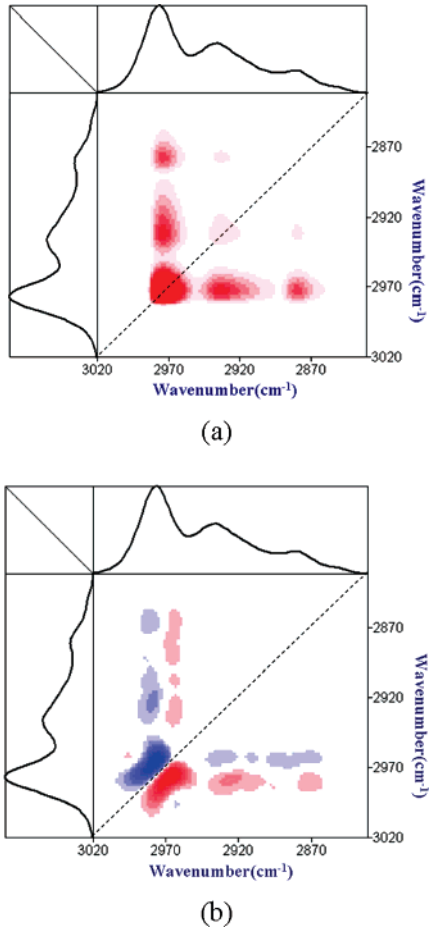

Figure 7. Synchronous (a) and asynchronous (b) maps of the PNIPAM 20 wt % D_2O solution in the region 3020−2830 cm^{-1} representing the cooling process.

hydrophilic groups, however, undergo transition until the temperature surpasses the LCST. Therefore, there is no doubt that the C−H groups are more heat-sensitive than the hydrophilic groups. To summarize, the complete microdynamics mechanism of the PNIPAM 20 wt % D_2O solution is concluded as: the CH_3 groups start the LCST phase separation with a two-step dehydration, the main chains follow by diffusion and aggregation, N−D and C═O groups then give up their hydrogen bonds with water, and finally the newly formed hydrogen bonds of C═O···D−N stabilize the globular state of the polymer chains. This sequence is illustrated clearly in Scheme 1. Because it is rather difficult to determine the number of the water molecules surround the methyl groups and form the "water cage", we use an approximate figure to denote the two-step dehydration process of the CH_3 groups in Scheme 1. Besides, as the hydrogen bonds between the limited HDO or incompletely deuterated −NH and carbonyl groups are so minim that we could neglect them and do not show them in Scheme 1.

Two-Dimensional Correlation Analysis of the Cooling Process

During cooling, 2D-IR spectroscopy method was also used to analyze the thermal behavior of the PNIPAM 20 wt % D_2O solution, and similar illations were done.

A. The C—H Region. Figure 7 represents the 2D-IR maps in the 3020−2830 cm^{-1} region gained in the cooling process of the PNIPAM 20 wt % D_2O solution. The autopeaks develop at 2970 and 2927 cm^{-1} in the synchronous map, pointing out great changes of both peaks with temperature dropping. The positive cross-peak at (2970, 2927) cm^{-1} in Figure 7a supports that the cooling-induced intensity variations of the peaks at 2970 and 2927 cm^{-1} take place in the same direction during cooling. In the asynchronous map of Figure 7b, the symbol of this cross-peak at (2970, 2927) cm^{-1} is also positive. According to Noda's[40−42] rule, both positive in the synchronous and asynchronous map, implies that the peak at 2970 cm^{-1} changes prior to the peak at 2927 cm^{-1}.

Another cross-peak at (2981, 2927) cm^{-1} could be identified negative in Figure 7b, and the symbol of this peak is judged to be positive in the slice spectrum of the synchronous map, different symbols in the synchronous and asynchronous maps prove that the peak at 2927 cm^{-1} changes before the one at about 2981 cm^{-1}.

The cross-peaks at (2970, 2927) and (2981, 2927) cm^{-1} in the 2D maps finally help to conclude the changing sequence of the observed bands as 2970 > 2927 > 2981 cm^{-1}. It has been known that the assignment of peak at 2970 and 2981 cm^{-1} is the vibration of methyl groups hydrated with less or more numbers of water molecules, respectively, therefore, the presence and the change sequence of the two peaks prove the two-step hydration process of the methyl groups during cooling, which is the reverse process of the dehydration effect of this groups in heating. This conclusion is consistent with the findings in the 1DIR analysis (Figure 2), that the dehydration or the hydration course of the hydrocarbon groups is a totally reversible process during the heating-and-cooling cycle.

With the whole event sequence obtained in Figure 7, 2970 > 2927 > 2981 cm^{-1}, it can be concluded that, during cooling, the CH_3 groups surrounded with fewer water molecules (2970 cm^{-1}) first hydrate with some heavy water, then some aggregated chains will disentangle, and finally the methyl groups will further hydrate with more water molecules, re-form the "water cage" structure, and finish the second step of hydration. However, compared with the conclusion of the heating process, we can easily see that there are some differences; the sequence in the cooling process is not contrary to the dynamic order in the heating course (2981 > 2970 > 2927 cm^{-1}).

B. The Amide I Region. One negative cross-peak at (1649, 1624) cm^{-1} exists in the synchronous 2D-IR spectrum (Figure 8a) of 1680−1580 cm^{-1}. As already known above, the peak at 1649 cm^{-1} is attributed to the vibrations of the C═O···D−N hydrogen bonds, and the peak at 1624 cm^{-1} is attributed to the C═O···D−O−D hydrogen bonds.[20,21,28] As a negative peak in the synchronous map, the cross-peak of (1649, 1624) cm^{-1} helps to infer that the two species of carbonyl hydrogen bonds transform in opposite directions during cooling, which is the same condition observed in heating (Figure 5a). In the asynchronous map of Figure 8b, this cross-peak of (1649, 1624) cm^{-1} is observed to be negative. With the help of Noda's rule[40−42] it can be inferred that the peak of 1649 cm^{-1} alters before that of 1624 cm^{-1} during cooling, which means the change of the hydrogen bonding of C═O···D−N is prior to that of C═O···D−O−D. The hydrogen bonds of C═O···D−N will first be destroyed, releasing the carbonyl groups, and the C═O groups will further form new hydrogen bonds with heavy water. Unlike the asynchronous map in the heating process (Figure 5b), there are not any other cross-peaks except for the peak at (1649, 1624) cm^{-1} in Figure 8b, which further validates the fact that the amounts of HDO and incompletely deuterated −NH (of PNIPAM) are rather limited, and the hydrogen bonds formed by them can be neglected.

C. Amide I Region vs the C—H Region. Similar to the heating process, this part of the analysis correlates the 1670−

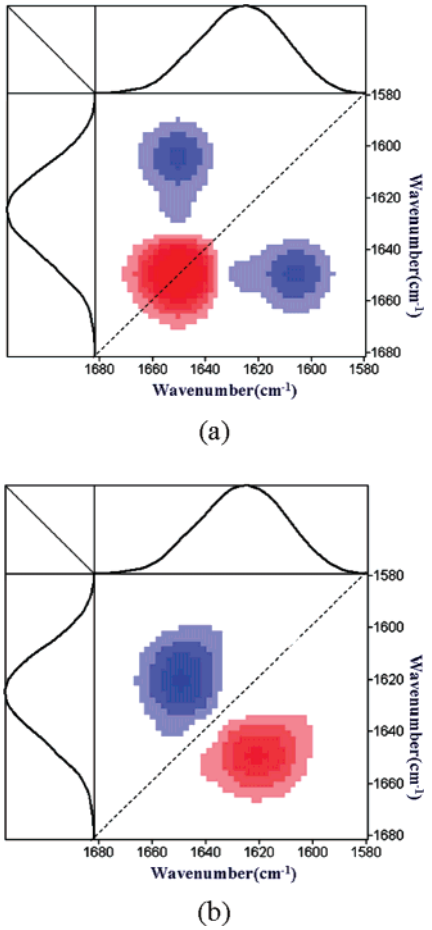

Figure 8. Synchronous (a) and asynchronous (b) maps of the PNIPAM 20 wt % D_2O solution in the region 1680−1580 cm^{-1} during the cooling process.

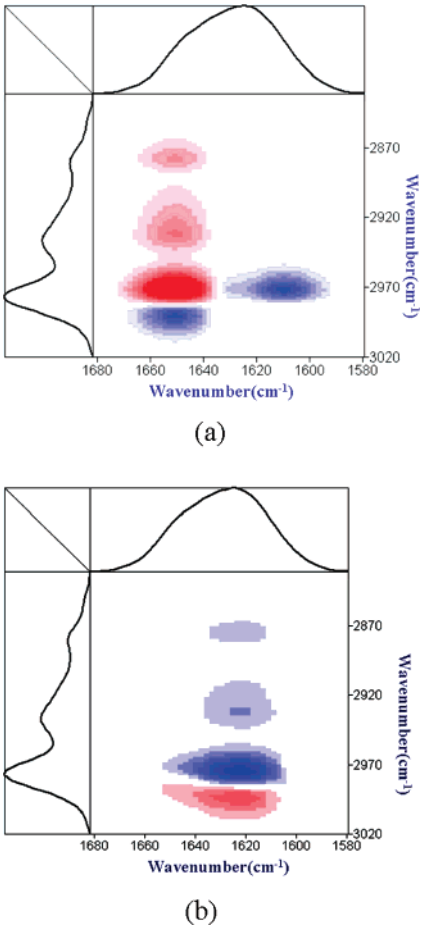

Figure 9. Synchronous (a) and asynchronous (b) maps of the PNIPAM 20 wt % D_2O solution in the regions 1680−1580 and 3020−2830 cm^{-1} during the cooling process.

1580 cm^{-1} region with the 3020−2830 cm^{-1} region (in Figure 9) and provides a macroscopic view of the whole cooling process of PNIPAM. The cross-peak at (1624, 2970) cm^{-1} can be observed in both 2D maps, and the symbol of this peak is both negative in the synchronous and asynchronous maps, thus we can infer 1624 > 2970 cm^{-1}. The sequence gained above in the 2D analysis of the CH region and the amide I during cooling is 2970 > 2927 > 2981 cm^{-1} and 1649 > 1624 cm^{-1}. Therefore, with the order we get in Figure 9 (1624 > 2970 cm^{-1}), the transition sequence of all the peaks can be linked as 1649 > 1624 > 2970 > 2927 > 2981 cm^{-1}. Other cross-peaks in Figure 9 can also prove this whole order.

Moreover, the information about the N−D groups should be also added to the former sequence. By using the spectra density method[57] mentioned above, the formation of the hydrogen bonds between N−H and water also happens faster than the formation of the C═O···H−O−H hydrogen bonds.[57] After release from C═O···D−N, the N−D groups could then form new hydrogen bonds with the heavy water molecules.

To make a summary, the dynamic changes take place in the PNIPAM 20 wt % D_2O solution is, as the temperature decreases, the intra- and interchain amide hydrogen bonds first break, the released N−D groups then form new hydrogen bonds with water immediately; the carbonyl groups interact with water and successively build their stable aqueous hydrogen-bonding structure. After that the CH_3 groups hydrate with a few water molecules, and finally some aggregated chains disentangle, which supports the second step of the hydration of the hydrophobic side-chain groups with more water molecules.

Conclusions

FTIR spectroscopic studies provide insight into the two primary aspects of the LCST behavior of PNIPAM 20% D_2O solution. As far as the hydrophobic groups are concerned, the quantitative analysis of the $\upsilon_{as}(CH_3)$ and $\upsilon_{as}(CH_2)$ peak positions proves the reversibility of their dehydration during heating. These peaks demonstrate red shifts during heating and return to their original high wavenumber positions when the temperature decreases. As for the hydrophilic groups, on the other hand, with temperature elevation, the hydrogen bonds between the C═O or N−D groups with water molecules are damaged and new intra- and interchain bonds between amide groups are formed. During the cooling process, the hydrogen bonds transform in the opposite direction. Regardless of its relationship to water, each part of the PNIPAM chain shows the "hysteresis" effect in the heating−cooling process. This phenomenon is caused by the hydrogen bonds between different overlapped segments in the collapsed state. Although the breakage of the C═O···D−N hydrogen bonds takes place during cooling, their great strength in the concentrated solution (20 wt %) prevents their total destruction even far below the LCST.

The 2D-IR method was used to explore the microdynamics mechanism of the phase separation of the PNIPAM aqueous solution. The sequence in the heating process can be written as: two-step dehydration of the CH_3 groups > main-chain aggregation > breakage of the N−D···O−D hydrogen bonds > dissociation of the C═O···D−O−D hydrogen bonds > formation of the C═O···D−N hydrogen bonds. The event order

of this system with decreasing temperature has also been investigated.

Acknowledgment. The authors gratefully acknowledge the financial support by the National Science of Foundation of China (NSFC) (Grants Nos. 20774022, 20573022, 20425415, 20490220), the "Leading Scientist" Project of Shanghai (Grant No. 07XD14002), the National Basic Research Program of China (Grant No. 2005CB623800) and Ph.D. Program of MOE (Grant No. 20050246010).

References and Notes

(1) Kanazawa, H.; Yamamoto, K.; Matsushima, Y.; Takai, N.; Kikuchi, A.; Sakurai, Y.; Okano, T. *Anal. Chem.* **1996**, *68*, 100.
(2) Shirota, H.; Kuwabara, N.; Ohkawa, K.; Horie, K. *J. Phys. Chem. B* **1999**, *103*, 10400.
(3) Kujawa, P.; Winnik, F. M. *Macromolecules* **2001**, *34*, 4130.
(4) Wang, X. H.; Wu, C. *Macromolecules* **1999**, *32*, 4299.
(5) Ding, Y. W.; Ye, X. D.; Zhang, G. Z. *Macromolecules* **2005**, *38*, 904.
(6) Van, Durme, K.; Van Assche, G.; Aseyev, V.; Raula, J.; Tenhu, H.; Van Mele, B. *Macromolecules* **2007**, *40*, 3765.
(7) Yim, H.; Kent, M. S.; Mendez, S.; Lopez, G. P.; Satija, S.; Seo, Y. *Macromolecules* **2006**, *39*, 3420.
(8) Plummer, R.; Hill, D. J. T.; Whittaker, A. K. *Macromolecules* **2006**, *39*, 8379.
(9) Ngai, T.; Auweter, H.; Behrens, S. H. *Macromolecules* **2006**, *39*, 8171.
(10) Rusu, M.; Wohlrab, S.; Kuckling, D.; Mohwald, H.; Schonhoff, M. *Macromolecules* **2006**, *39*, 7358.
(11) Yuan, G. C.; Wang, X. H.; Han, C. C.; Wu, C. *Macromolecules* **2006**, *39*, 6207.
(12) Kujawa, P.; Aseyev, V.; Tenhu, H.; Winnik, F. M. *Macromolecules* **2006**, *39*, 7686.
(13) Kujawa, P.; Segui, F.; Shaban, S.; Diab, C.; Okada, Y.; Tanaka, F.; Winnik, F. M. *Macromolecules* **2006**, *39*, 341.
(14) Kujawa, P.; Tanaka, F.; Winnik, F. M. *Macromolecules* **2006**, *39*, 3048.
(15) Qin, S. H.; Geng, Y.; Discher, D. E.; Yang, S. *Adv. Mater.* **2006**, *18*, 2905.
(16) Kobayashi, J.; Kikuchi, A.; Sakai, K.; Okano, T. *Anal. Chem.* **2003**, *75*, 3244.
(17) Kaholek, M.; Lee, W. K.; LaMattina, B.; Caster, K. C.; Zauscher, S. *Nano Lett.* **2004**, *4*, 373.
(18) Corkhill, P. H.; Jolly, A. M.; Ng, C. O.; Tighe, B. J. *Polymer* **1987**, *28*, 1758.
(19) Barnes, A.; Corkhill, P. H.; Tighe, B. J. *Polymer* **1988**, *29*, 2191.
(20) Cheng, H.; Shen, L.; Wu, C. *Macromolecules* **2006**, *39*, 2325.
(21) Maeda, Y.; Higuchi, T.; Ikeda, I. *Langmuir* **2000**, *16*, 7503.
(22) Stillinger, F. H. *Science* **1980**, *209*, 451.
(23) Jacob, Israelachvili, R. P. *Nature (London)* **1982**, *300*, 341.
(24) Inomata, H.; Goto, S.; Saito, S. *Macromolecules* **1990**, *23*, 4887.
(25) Otake, K.; Inomata, H.; Konno, M.; Saito, S. *Macromolecules* **1990**, *23*, 283.
(26) Cho, E. C.; Lee, J.; Cho, K. *Macromolecules* **2003**, *36*, 9929.
(27) Heskins, M.; Guillet, J. E. *J. Macromol. Sci. Chem.* **1968**, *A2*, 1441.
(28) Maeda, Y.; Higuchi, T.; Ikeda, I. *Langmuir* **2001**, *17*, 7535.
(29) Maeda, Y.; Yamamoto, H.; Ikeda, I. *Langmuir* **2001**, *17*, 6855.
(30) Shibayama, M.; Suetoh, Y.; Nomura, S. *Macromolecules* **1996**, *29*, 6966.
(31) Schild, H. G.; Tirrell, D. A. *J. Phys. Chem.* **1990**, *94*, 4352.
(32) Inomata, H.; Goto, S.; Otake, K.; Saito, S. *Langmuir* **1992**, *8*, 687.
(33) Winnk, F. M. *Macromolecules* **1990**, *23*, 233.
(34) Walter, R.; Ricka, J.; Quellet, C.; Nyffenegger, R.; Binkert, T. *Macromolecules* **1996**, *29*, 4019.
(35) Fujishige, S.; Kubota, K.; Ando, I. *J. Phys. Chem.* **1989**, *93*, 3311.
(36) Ohta, H.; Ando, I.; Fujishige, S.; Kubota, K. *J. Polym. Sci., Polym. Phys.* **1991**, *29*, 963.
(37) Terada, T.; Inaba, T.; Kitano, H.; Maeda, Y.; Tsukida, N. *Macromol. Chem. Phys.* **1994**, *195*, 3261.
(38) Katsumoto, Y.; Tanaka, T.; Sato, H.; Ozaki, Y. *J. Phys. Chem. A* **2002**, *106*, 3429.
(39) Katsumoto, Y.; Tanaka, T.; Ozaki, Y. *Macromol. Symp.* **2004**, *205*, 209.
(40) Noda, I. *Appl. Spectrosc.* **1993**, *47*, 1329.
(41) Noda, I. *Appl. Spectrosc.* **2000**, *54*, 994.
(42) Noda, I.; Story, G. M.; Marcott, C. *Vibr. Spectrosc.* **1999**, *19*, 461.
(43) Wu, P.; Siesler, H. W. *J. Mol. Struct.* **2000**, *521*, 37.
(44) Segtnan, V. H.; Sasic, S.; Isaksson, T.; Ozaki, Y. *Anal. Chem.* **2001**, *73*, 3153.
(45) Shen, Y.; Wu, P. Y. *J. Phys. Chem. B* **2003**, *107*, 4224.
(46) Sasic, S.; Amari, T.; Ozaki, Y. *Anal. Chem.* **2001**, *73*, 5184.
(47) Jonsson, J.; Persson, P.; Sjoberg, S.; Lovgren, L. *Appl. Geochem.* **2005**, *20*, 179.
(48) Lopez-Diez, E. C.; Winder, C. L.; Ashton, L.; Currie, F.; Goodacre, R. *Anal. Chem.* **2005**, *77*, 2901.
(49) Shirota, H.; Endo, N.; Horie, K. *Chem. Phys.* **1998**, *238*, 487.
(50) Shirota, H.; Horie, K. *Chem. Phys.* **1999**, *242*, 115.
(51) Shirota, H.; Ohkawa, K.; Kuwabara, N.; Endo, N.; Horie, K. *Macromol. Chem. Phys.* **2000**, *201*, 2210.
(52) Shirota, H.; Horie, K. *Macromol. Symp.* **2004**, *207*, 79.
(53) Shibayama, M.; Tanaka, T.; Han, C. C. *J. Chem. Phys.* **1992**, *97*, 6829.
(54) Sun, B. J.; Lin, Y. N.; Wu, P. Y. *Appl. Spectrosc.* **2007**, *61*, 765.
(55) Schmidt, P.; Dybal, J.; Trchova, M. *Vibr. Spectrosc.* **2006**, *42*, 278.
(56) Noda, I.; Ozaki, Y. *Two-dimensional Correlation Spectroscopy: Applications in Vibrational and Optical Spectroscopy*; Chichester: West Sussex, England, and John Wiley & Sons: Hoboken, NJ, 2004.
(57) Tamai, Y.; Tanaka, H.; Nakanishi, K. *Macromolecules* **1996**, *29*, 6761.

MA702062H